Analysis of the Electric Field Distribution in a Wire-Cylinder Electrode Configuration

Konstantinos N. Kiousis, Antonios X. Moronis and Wolf G. Früh
Technological Educational Institute of Athens
Energy Technology Department
Athens, Greece
konstantinosq@gmail.com, amoronis@teiath.gr, w.g.fruh@hw.ac.uk

***Abstract*— The electric field distribution in an air gap between a wire-cylinder electrode configuration, has been studied by implementing Finite Element Analysis. The electrodes were assumed to be surrounded by air at normal conditions, while high dc voltage has been applied across them, with positive polarity at the wire. Numerical analysis on the maximum electric field intensity along the wire-cylinder gap axis, as well as on the potential distribution in the air surrounding the electrodes has been carried out, considering different geometrical characteristics of the electrodes. The applied mesh parameters were optimized, in terms of accuracy and processing power. The maximum field intensity was mainly associated with the wire radius r and the electrode gap length d. The cylindrical electrode radius R had a limited impact on the maximum electric field intensity but, on the other hand, it had a strong effect in the distribution of the electric field lines. Finally, a formula for the estimation of the maximum electric field intensity is proposed.**

Keywords*— *finite element methods; HV electrodes; modeling; numerical analysis

I. INTRODUCTION

The study of the electric field strength distribution is of great importance for the design and dimensioning of high voltage equipment [1] - [3]. The electric field strength is the key parameter that defines the behavior of insulating materials under high electric field stress. There are numerous applications of high voltage technology in power electrical systems, in industry and research. The experimental measurement of the field strength in air gaps is in fact difficult and not quite accurate, due to the presence of sensing elements which may affect the distribution of the electric field. On the other hand, computer methods can provide instant and accurate results and are capable of solving problems in more complex conditions. Some of the most commonly used software applications implement the Finite Element Analysis (FEA). FEA modeling in electrostatics is based on the application of a set of differential equations that describe the problem, considering certain boundary conditions, in order to come to a unique solution. FEA modeling breaks the problem down into a large number of regions, each with a simple geometry (e.g. triangles), defined by a mesh with a very large number of nodes. Then the problem is transformed from a small but difficult to solve problem into a big but relatively easy to solve problem, involving a very large number of unknown quantities.

Despite the large number of computational studies of the electric field distribution in uniform and non-uniform electric fields at different electrode configurations (e.g. parallel planes, tip-plane, concentric cylinders, wire-wire etc.) found in literature [4] - [10], there is no study available for the wire-cylinder electrode arrangement. On the other hand, experimental investigations, by means of corona discharge current [11], [12] and current distribution [13], have already been conducted for wire-cylinder electrode pairs.

The goal of this paper is the fine modeling and analysis of the electric field strength in a wire-cylinder electrode arrangement in atmospheric air at normal conditions, considering the geometrical characteristics of the electrodes. In this study the wire radius r ranged from *1* to *500μm*, the cylinder radius R from *1* to *20mm* and the gap d between the electrodes ranged from *1* to *10cm*. These dimensions are quite common in experimental studies of corona discharge currents and the corresponding electro-hydrodynamic (*EHD*) effects, which can be found in bibliography [11] - [13]. This analysis was based on FEA techniques. On this purpose, open source FEA modeling software *F.E.M.M.* ver. 4.2 has been implemented. The mesh parameters have been fully investigated in order to optimize the applied mesh around the specific areas of interest, such as the inter-electrode region and especially at points along the line defining the shortest distance d between the electrodes, thus ensuring the accuracy of the results.

II. GOVERNING EQUATIONS

In our case we have a typical electrostatics problem which is governed by the well-known Gauss's and Poisson's equations, assuming homogenous field and steady state conditions [1]-[3]:

$$E = -\nabla V \tag{1}$$

$$\nabla^2 V = -\rho / \varepsilon_0 \tag{2}$$

where E is the electric field intensity, V is the applied voltage, ρ is the space charge density and ε_0 is the dielectric permittivity of air. The electric field should satisfy the charge conservation law:

$$\nabla \cdot j = 0 \quad (3)$$

where j is the current density. The latter is defined as:

$$j = \rho \cdot u = \rho \cdot \mu \cdot E \quad (4)$$

where u is the ion drift velocity and μ is the ion mobility. (1), (2), (3) and (4) can be combined to obtain:

$$\nabla\left\{\left(\nabla^2 V\right)\left(\nabla V\right)\right\} = 0 \quad (5)$$

In theory, the physical problem is reduced to the mathematical problem of solving (5) with the appropriate boundary conditions. The FEA model provides numerical results for the voltage distribution at each node of the applied mesh. The electric field strength may then be easily determined by (1) around the user-defined domain, where the mesh is constructed. In such a computational analysis, the solver precision, the boundary conditions, the bounding box size defining the domain and the mesh distribution are of great importance for the accuracy of the results [14]-[18].

III. Electrode Geometry

The wire-cylinder electrode pair under consideration is shown in Fig. 1. A thin cylindrical wire of radius r is placed parallel to a cylinder with significantly larger radius R, at distance d. The wire radius r, the cylinder radius R and the air gap d between the electrodes are critical parameters which define the geometry and, in this way, determine the electric field strength. In this study, r was ranging between *1* and *500μm*, R between *1* and *20mm*, while the gap d between the electrodes was ranging between *1* and *10cm*. In addition, it has been assumed that positive potential has been applied to the wire while the cylinder is grounded.

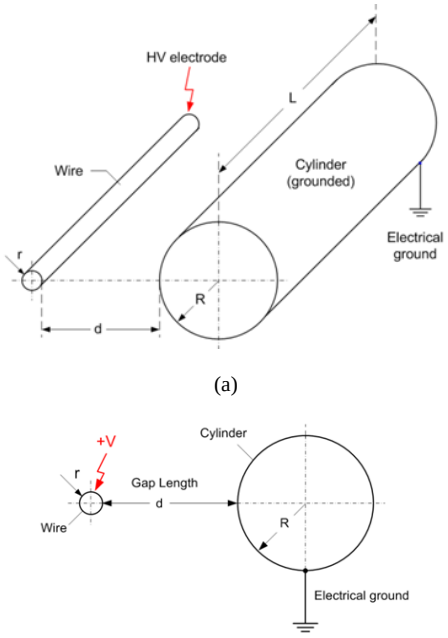

Fig. 1. (a) Perspective plan of the electrodes arrangement in space and (b) simplified planar model, due to longitudinal axis symmetry.

Theoretically, these electrodes may have infinite length, but due to the longitudinal axis symmetry, the electric field or potential distribution may only change in the radial direction, perpendicular to the wire or the cylinder surface, along the gap. Therefore, this three-dimensional problem may be minimized into a two-dimensional problem that requires a much smaller number of nodes and less computing power.

IV. Modeling Parameters

F.E.M.M. solves (5) for the potential V, over the user defined domain with the user defined sources and boundary conditions. It discretizes the problem domain using triangular elements, which form a mesh consisting of a large number of nodes. The solution over each element is approximated by a linear interpolation of the values of potential at the three vertices of the triangle [19]. In our case, a two-dimensional planar electrostatic problem was defined with a solver precision 10^{-8}.

Due to the symmetry of the electrode geometry along the gap axis, half-plane modeling has been applied. The problem's domain was defined by the bounding box shown in Fig. 2. This box sets the limits of the surrounding dielectric medium, which in our case was atmospheric air. The bounding box size was defined by the fixed distances $A=k \cdot D$ between its sides and the electrodes, where $D=2r+d+2R$ was the total length of the electrodes assembly (air gap included) and k was a scaling constant.

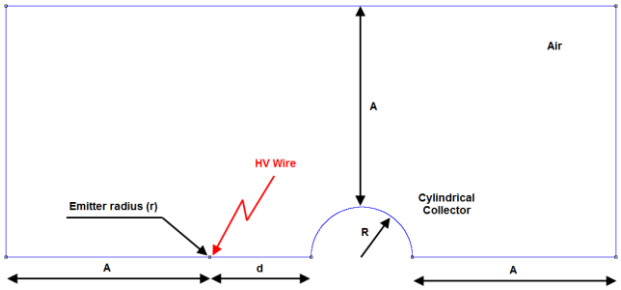

Fig. 2. The model of the two electrodes and the bounding box of the surrounding air, where the mesh is applied.

The determination of the bounding box size is generally critical, since a small box may affect the electric field distribution and lead to errors, or, on the other hand, a large box may unnecessarily lead to a very large number of nodes, demanding more processing power. Preliminary analysis with different k values, has shown that a suitable choice would be $k=3$ [20]. This value had been kept constant throughout all simulations.

Dirichlet conditions [21] were explicitly defined on the problem's boundaries. The wire and cylinder outer surfaces were considered to be equipotentials with fixed voltages *1kV* and *0V*, respectively. Subsequently, all electric field strength results were defined per *kV* of the applied voltage. Since the applied voltage may vary in practice, valid results may be easily obtained in any case, by just multiplying the electric field strength at *1kV*, by the number of applied kilovolts. This can be easily explained by (1). For example, considering any fixed pair of wire-cylinder electrodes with *1kV* voltage

difference, then, if $V_1(x,y)$ is the potential and $E_1(x,y)$ is the corresponding electric field strength at any point (x,y), then, at αkV, the potential would be $V_a(x,y)=aV_1(x,y)$ and the corresponding electric field strength $E_a(x,y)$ could be determined by (1) as follows:

$$E_a(x,y) = -\nabla V_a(x,y) = -\nabla\left(a \cdot V_1(x,y)\right) = \\ = a \cdot \left(-\nabla V_1(x,y)\right) = a \cdot E_1(x,y) \quad (6)$$

It becomes clear that the electric field strength at αkV equals α times the electric field at *1kV*.

There is a set of key parameters to the *F.E.M.M.* model so as to ensure proper mesh formation. The mesh discretization at distances very close to the electrode surfaces depends mainly on two parameters, the maximum arc segment degrees and the minimum angle. These determine the size of the triangular elements near the outer surface of the electrodes, where the electric field and voltage gradients get their maximum values, thus demanding very fine analysis by a dense mesh. On the other hand, the mesh distribution along the gap is a function of the local element size along line parameter. The density of the mesh elements in other areas such as the inter-electrode space away from the electrode surfaces are functions of another key parameter, the mesh size.

Analytical study of the influence of each one of the mesh parameters has been carried out, by running a large number of simulations, using different *maximum arc segment angles*, *minimum angles of the triangular mesh*, *local elements size along line* and *mesh sizes*, in order to accomplish convergence of the results. In this way an optimal mesh has been configured, in terms of accuracy and processing power consumption, with the key parameter values given in Table 1. An example of the optimized mesh is shown in Fig. 3 for a wire-cylinder electrode setup with $r=25\mu m$, $R=15mm$ and $d=3cm$. The mesh is denser in the areas of interest, i.e. near the high voltage and the grounded electrode, as well as along the gap axis.

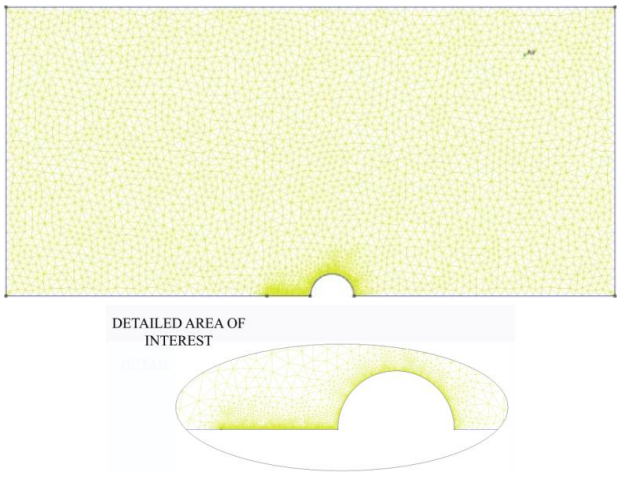

Fig. 3. Optimized mesh layout and detailed area of interest. Wire-cylinder electrode configuration with geometrical parameters: $r=25\mu m$, $R=15mm$ and $d=3cm$. Here *A=3D*.

TABLE I. COMPARISON BETWEEN THE DEFAULT VALUES OF THE F.E.M.M. KEY PARAMETERS AND THE SELECTED OPTIMIZED VALUES

FEMM key parameter	Default values	Selected values (optimized)
Minimum Angle (degrees)	30	31
Maximum Arc Segment (degrees)	5	0.5
Local Element Size Along Line (μm)	auto	10
Mesh Size (μm)	auto	auto
Nodes	3632	22523
Elements	6906	41026

For verification purposes, the optimized mesh has been used in order to estimate the maximum field intensity E_{max}, at well-known geometries, similar to the wire-cylinder pair, such as two identical cylindrical conductors in parallel (where $r/R=1$), for which analytical formulas can be found in bibliography. In this way, the accuracy of the optimized mesh could be easily tested. In the case of two parallel cylindrical conductors E_{max} is given by the analytical formula [14]:

$$E_{\max} = \frac{V}{d} \cdot \frac{\sqrt{\left(d/2r\right)^2 + \left(d/r\right)}}{\ln\left(1 + \left(d/2r\right) + \sqrt{\left(d/2r\right)^2 + \left(d/r\right)}\right)} \quad (7)$$

where V is the applied voltage, d is the distance between the two electrodes and r is the electrode radius.

F.E.M.M. simulations, that have been conducted with the optimized mesh for two parallel cylindrical wires with r and d values within the limits of our study ($r=1\text{-}500\mu m$ and $d=1\text{-}10cm$), have provided results which are in good agreement with theoretical expectations, in all cases. Such results are given in Table 2, where both theoretical and simulation values for E_{max} are shown, along with the corresponding relative error.

TABLE II. COMPARISON BETWEEN THE ELECTRIC FIELD INTENSITY (THEORETICAL AND *F.E.M.M.* RESULTS) FOR TWO IDENTICAL PARALLEL CONDUCTORS AT *1KV* POTENTIAL DIFFERENCE

r(μm)	d(cm)	Theoretical E_{max} (V/m)	Optimized Mesh results E_{max} (V/m)	Relative error (%)
1	1	$54{,}296 \cdot 10^6$	$54{,}183 \cdot 10^6$	0.21
25	3	$2{,}825 \cdot 10^6$	$2{,}803 \cdot 10^6$	0.78
100	5	807250	799771	0.93
250	7	357014	353483	0.99
500	10	190261	187465	1.47

V. Simulation Results For The Wire-Cylinder Electrodes

As expected, the simulation results have shown that the maximum electric field strength E_{max} is located at the outer surface of the wire electrode, at the least distant point from the cylinder (see Fig. 4a, 5a and 6), while the minimum field strength E_{min} has been identified at distance x, depending on the R/r ratio (see Fig. 6).

On the other hand, the potential distribution across the electrode gap d is shown in Fig. 4b and 5b, where it becomes clear that equipotentials are in fact cylindrical surfaces with displaced centers along the gap axis.

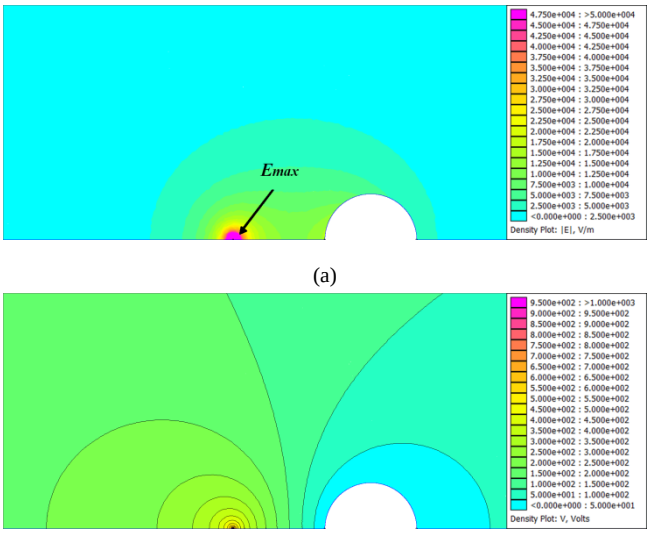

(a)

(b)

Fig. 4. (a) Electric field strength and (b) potential distribution. Wire-cylinder electrodes with *r=25μm*, *R=15mm* and *d=3cm*, at *1kV* potential difference.

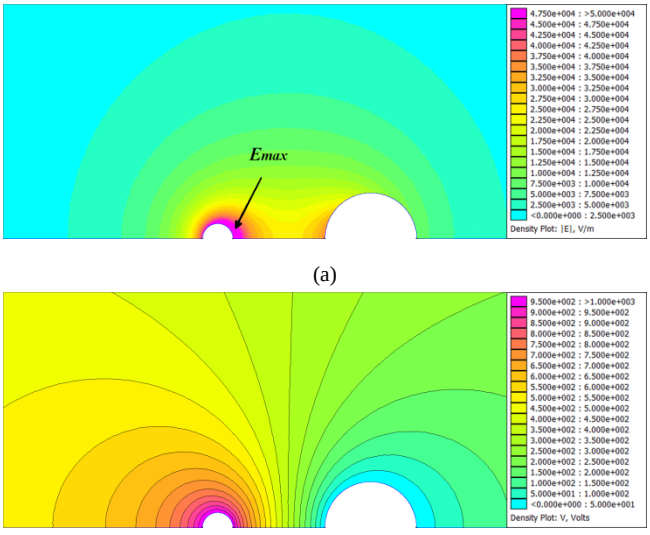

(a)

(b)

Fig. 5. (a) Electric field strength and (b) potential distribution. Wire-cylinder electrodes with *r=5mm*, *R=15mm* and *d=3cm*, at *1kV* potential difference.

The variation of the electric field intensity across the gap, for different R/r ratios is given in Fig. 6, where the normalized field $E(x)/E_{max}$ is shown, at distance x from the wire's surface, expressed as a percentage of the total electrode gap length d. It can be seen that the field intensity gets its maximum value at the wire's surface (where $x=0$ or $x/d=0\%$) then diminishes along the gap until its minimum value and, finally, increases at a certain level depending on the R/r ratio, at the cylinder's surface (where $x=d$ or $x/d=100\%$). From another point of view, R/r ratio may be considered as a measure of the electric field inhomogeneity, since larger R/r ratios result in a more inhomogeneous field distribution along the gap (see Fig. 6).

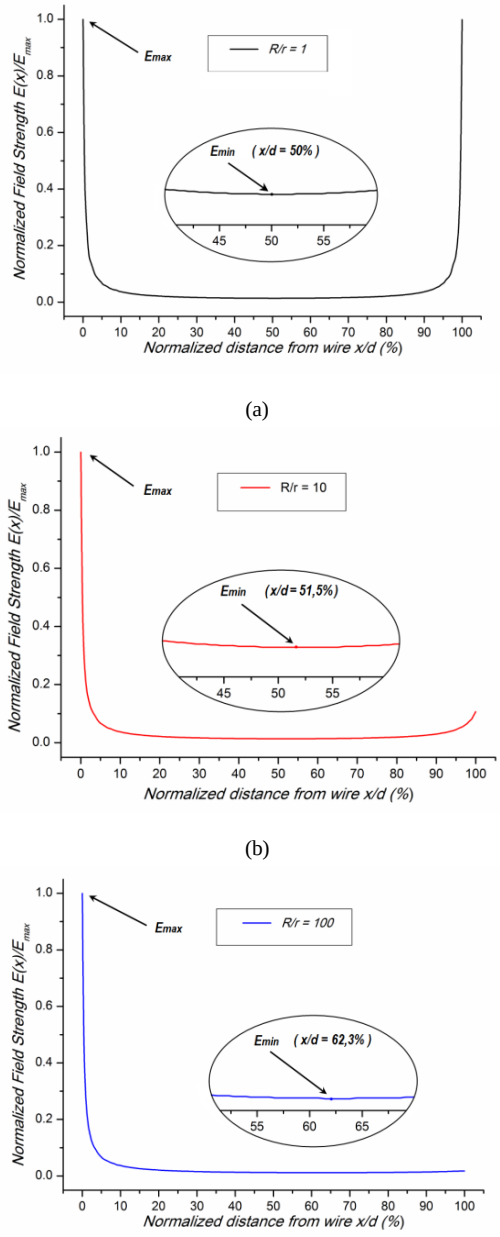

(a)

(b)

(c)

Fig. 6. Normalized electric field intensity along the gap axis, and detail where E_{min} is shown. In this case *r=100μm*, *d=3cm* and (a) *R/r=1*, (b) *R/r=10* and (c) *R/r=100*. Similar results can be obtained for different *d* and *r* values as well..

The dependence of the maximum electric field intensity E_{max} on the wire radius r, the cylinder radius R and the electrode gap d has also been examined. Fig. 7 shows typical curves of E_{max} versus d/r ratio for, for different gaps d and cylinder radii R, while Fig. 8 shows the variation of E_{max} versus d/R ratio for different wire radii r gaps d. From these results, it becomes clear that E_{max} is strongly affected by the d/r ratio, in a linear way, and secondly, by the d/R, ratio.

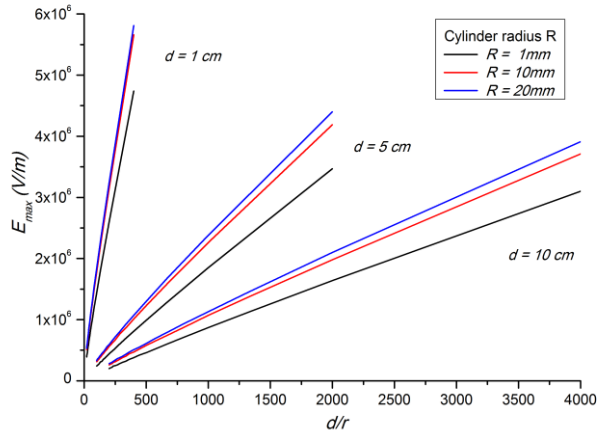

Fig. 7. Variation of E_{max} with the d/r ratio. Electrode gap at *1cm*, *5cm* and *10cm* and potential difference *1kV* in all cases.

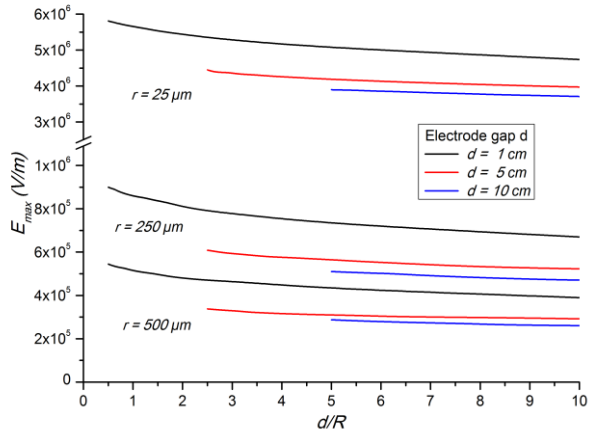

Fig. 8. E_{max} variation with the d/R ratio. Wire radius at *25μm*, *250μm* and *500μm* and potential difference at *1kV* in all cases.

Gap distance d remains a critical parameter in all cases. Generally, maximum electric field intensities can be reached by using thin wires, small electrode separation gaps and large cylinder radii, which is a reasonable finding, since the electric field distribution is thus becoming strongly inhomogeneous.

On the other hand, Fig. 9 and Fig. 10 show how the minimum field strength E_{min} along the gap axis, is affected by d/r, d/R and the electrode gap d. Here it seems that the gap distance d is the dominant parameter, while the wire radius r comes next.

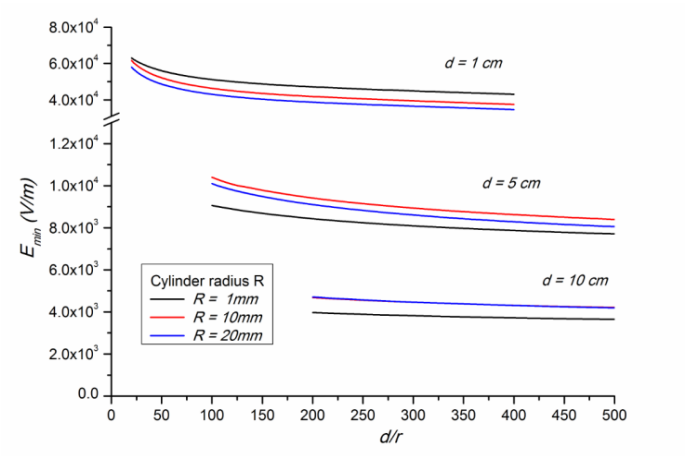

Fig. 9. Variation of E_{min} with the d/r ratio. Electrode gap at *1cm*, *5cm* and *10cm* and potential difference at *1kV* in all cases.

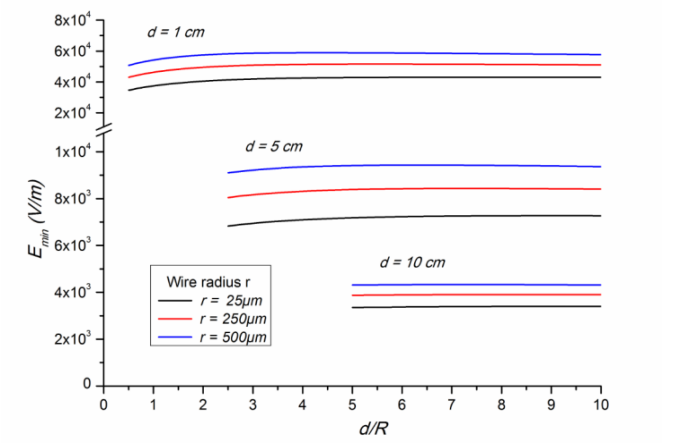

Fig. 10. E_{min} variation with the d/R ratio. Wire radius at *25μm*, *250μm* and *500μm* and potential difference at *1kV* in all cases.

VI. Proposed Formula For E_{MAX} In The Case Of A Wire-Cylinder Electrode Arrangement

According to simulation results, E_{max} increases linearly with d/r ratio. On the other hand, it is also dependent on the d/R ratio. The gap distance d is found to be critical in determining the electric field in all cases. This comes in agreement with theoretical expectations, since the ratio V/d is frequently used in bibliography as a standard measure of the mean value of the electric field strength in any gap [22] - [26]. Besides, most of the formulas for E_{max} in well-known geometries are usually expressed as the product of V/d by a geometrical constant, as in (7) [1] - [3]. According to the above, an effort has been made to introduce a formula for the maximum electric field strength E_{max} in the wire-cylinder arrangement.

Detailed analysis of all simulation results has shown that the maximum electric field intensity $E_{maxW\text{-}C}$ within the limits of this study can be approximated by the following formula:

$$E_{\max W-C} = \frac{V}{d} \cdot \frac{\gamma_1}{\ln\left[\gamma_1\left(\gamma_2+2\right)\right]} \tag{8}$$

where $V(V)$ is the applied voltage, $\gamma_1=d/r$ and $\gamma_2=d/R$ (dimensionless factors).

On the other hand, similarly defining $\gamma'=d/2r$ in (7), we have:

$$E_{\max}=\frac{V}{d}\cdot\frac{\sqrt{\gamma'(\gamma'+2)}}{\ln\left[(\gamma'+1)+\sqrt{\gamma'(\gamma'+2)}\right]} \quad (9)$$

It should be noted that in the case of two identical cylindrical conductors in parallel $r=R$ ($\gamma_1=\gamma_2=\gamma$) and for $d>>r$ we have $\gamma>>1$, $\gamma+2\approx\gamma$.

Then (8) becomes:

$$E_{\max}=\frac{V}{d}\cdot\frac{\gamma}{2\cdot\ln(\gamma)} \quad (10)$$

In fact (10) equals (9) for $d>>r$, since $\gamma'>>1$, $\gamma'+1\approx\gamma'$ and $\gamma'+2\approx\gamma'$ (also considering that $\gamma'=\gamma/2$).

VII. Discussion

The results of (8) for all possible combinations of the critical geometrical parameters r, R and d, within the limits of this study ($r\le 500\mu m$, $R\ge 1mm$ and $d\ge 1cm$), are in good agreement with the corresponding maximum field intensity E_{max} values estimated by the *FEA* simulation.

Typical graphs of the change in relative error for E_{max} with the geometrical parameters r, R and d are given in Fig. 11. These graphs show that the error diminishes as d and R increase with respect to the wire radius r.

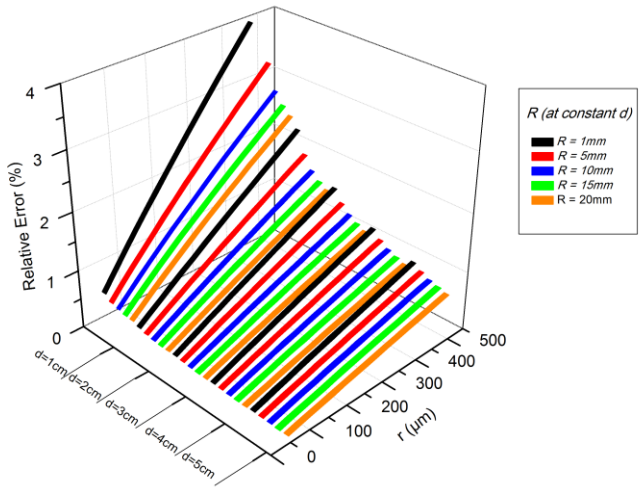

Fig. 11. Representation of the relative error between simulated data and the empirical formula results for E_{max} according to (8).

According to Fig. 11, the relative error remains small, below 4 % (worst case) and decreases with increasing gap and cylinder radius.

Practically speaking, the proposed formula for E_{max} can be effectively used for electrode pairs constructed by thin wires parallel to cylinders of considerably larger radii at distances of a few centimeters or more. Such electrode arrangements have been used in previous work [11]-[13] and are suitable for corona or ionic wind applications, due to the high inhomogeneity of the produced electric field. The determination of the maximum electric field in these cases is always one of the most critical design parameters.

Moreover, the electric field utilization factor $n=E_{av}/E_{max}$, ($E_{av}=V/d$), which is frequently used to indicate the electric field inhomogeneity [27], can be easily defined from (8) as:

$$n_{W-C}=\frac{\ln\lfloor\gamma_1(\gamma_2+2)\rfloor}{\gamma_1} \quad (11)$$

VIII. Conclusions

The electric field distribution in a typical wire-cylinder electrode configuration in air, under high voltage dc application has been studied with the aid of dedicated simulation software implementing the *Finite Element Analysis*.

The applied mesh parameters have been optimized and validated, in order to ensure the accuracy of the results. The maximum electric field strength E_{max}, as well as the minimum electric field strength E_{min}, has been examined, considering geometrical characteristics of the electrodes such as the wire radius r, the electrode spacing d and the cylindrical electrode radius R.

Simulations have shown that E_{max} is mainly associated with the wire electrode radius r. Generally, smaller wire radii result in higher field intensities around the wire, especially at the wire's surface, where E_{max} is observed. In addition, E_{max} was found to be inversely proportional to the electrode gap d.

Moreover, larger cylinder radii R lead to higher E_{max} values, for constant r and d. On the other hand, E_{min} is strongly related to the electrode gap d, while the wire radius r and the cylindrical electrode radius R have a limited impact on the minimum electric field intensity.

Finally, an empirical formula for the estimation of the maximum electric field intensity has been proposed. The correlation of the simulated data with the empirical formula results was found to be satisfactory, with an absolute error lower than 4% in all cases.

References

[1] M. Khalifa, High-Voltage Engineering Theory and Practice, New York: Marcel Dekker Inc., 1990.

[2] M.S. Naidu, V. Kamaraju, High Voltage Engineering, New York: Mc Graw Hill, 1996.

[3] C.L. Wadhwa, High Voltage Engineering, New Age International (P) Ltd., 2007.

[4] K. Hidaka, T. Kouno, "A method for measuring electric field in space charge by means of pockels device", Journal of Electrostatics, 11, 1982, pp. 195-211.

[5] I.W. McAllister, "Electric fields and electrical insulation", Dielectrics and Electrical Insulation, IEEE Transactions, 9, 2002, pp. 672-696.

[6] A. Maglaras, L. Maglaras, "Modeling and analysis of electric field distribution in air gaps, stressed by breakdown voltage", Math. Methods and Computational Techniques in Electrical Engineering (MMACTEE), WSEAS, Athens, 2004.

[7] A. Maglaras, "Numerical Analysis of Electric Field in Air Gaps, Related to the Barrier Effect", 1st International Conference 'From Scientific Computing to Computational Engineering' Athens, 2004.

[8] J. Mackerle, "Finite element and boundary element modelling of surface engineering systems: A bibliography (1996–1998)", Finite Elements in Analysis and Design, 34, 2000, pp. 113-124.

[9] M. Rezouga, A. Tilmatine, R. Ouiddir, K. Medles, "Experimental Modelling of the Breakdown Voltage of Air Using Design of Experiments", Journal of Advances in Electrical and Computer Engineering, 9, 1, 2009, pp. 41-45.

[10] M. Rau, A. Iftemie, O. Baltag, D. Costandache, "The Study of the Electromagnetic Shielding Properties of a Textile Material with Amorphous Microwire", Journal of Advances in Electrical and Computer Engineering, 11, 1, 2011, pp. 17-22.

[11] K.N. Kiousis, A.X. Moronis, "Experimental Investigation of EHD Flow in Wire to Cylinder Electrode Configuration", EUROPES Power and Energy Systems, IASTED, Crete, pp. 21-26, 2011.

[12] K. Kantouna, G.P. Fotis, K.N. Kiousis, L. Ekonomou, G.E. Chatzarakis, "Analysis of a Cylinder-Wire-Cylinder Electrode Configuration during Corona Discharge", Circuits, Systems, Communications, Computers and Applications (CSCCA), WSEAS, Iasi, pp. 204-208, 2012.

[13] R.D. Morrison, D.M. Hopstock, "The distribution of current in wire-to-cylinder corona", Journal of Electrostatics, 6, 1979, pp. 349-360.

[14] E. Kuffel, W.S. Zaengl, J. Kuffel, High Voltage Engineering Fundamentals, Newnes Oxford, 2000.

[15] P.P. Sylvester, R.L. Ferrari, Finite Elements for Electrical Engineers 3rd Edition, New York: Cambridge University Press, 1996.

[16] J. Jin, Finite Element Method in Electromagnetics 2nd Edition, New York: Wiley-IEEE Press, 2002.

[17] S.S. Rao, The Finite Element Method in Engineering, Boston: Butterworth-Heinemann, 1999.

[18] J. Mackerle, "Mesh generation and refinement for FEM and BEM— A bibliography (1990–1993)", Finite Elements in Analysis and Design, 15, 1993, pp. 177-188.

[19] D. Meeker, Finite Element Method Magnetics (F.E.M.M.) Ver 4.2 User's Manual, 2010.

[20] K.N. Kiousis, A.X. Moronis, "Modeling and Analysis of the Electric Field and Potential Distribution in a Wire-Cylinder Air Gap", Computer Engineering and Applications (CEA '13), WSEAS, Milan, pp. 35-40, 2013.

[21] I. Hlavacek, M. Krizek, "On a super convergent finite element scheme for elliptic systems. I. Dirichlet boundary condition", Applications of Mathematics, 32, 1987, pp. 131-154.

[22] T. Matsumoto, "DC corona loss of coaxial cylinders", Electr. Eng. Japan, 88, 1968.

[23] P. Giubbilini, "The current-voltage characteristics of point-to-ring corona", Journal of Applied Physics, 64, 1988.

[24] R.T. Waters, T. S. Rickard, W.B. Stark, "The Structure of the Impulse Corona in a Rod/Plane Gap I The Positive Corona", Proc. R. Soc., 1970, pp. 1-25.

[25] G.F. Ferreira, O.N. Oliveira, J.A. Giacometti, "Point-to-plane corona: Current-voltage characteristics for positive and negative polarity with evidence of an electronic component", Journal of Applied Physics, 59, 1996, pp. 3045-3049.

[26] F. Carreno, E. Bernabeu, "On wire-to-plane positive corona discharge", Journal of Physics D: Appl. Physics, 27, 1994.

[27] R. Arora, W. Mosch, High Voltage and Electrical Insulation Engineering, New Jersey: John Wiley and Sons Inc., 2011.